

A Perturbative Lambda Formulation

A. Dadone* and M. Napolitano†
Università di Bari, Bari, Italy

This paper provides a new perturbative lambda formulation for the numerical solution of compressible flows. The time-dependent Euler equations are recast into compatibility equations for perturbative bicharacteristic variables that are the differences between the standard Riemann variables and those corresponding to an appropriate steady incompressible flow. In this way, the geometry-induced gradients are accounted for by the incompressible flow solution and the smooth correction accounting for compressibility effects is solved accurately even on a coarse mesh. The new perturbative lambda equations for two-dimensional homentropic flows are provided in a general orthogonal curvilinear coordinate system and solved numerically by means of an alternating direction implicit method. Results are presented for flow past a NACA 0012 airfoil that demonstrate the remarkable accuracy of the proposed methodology.

Introduction

THIS paper is concerned with the numerical simulation of compressible inviscid flows up to the weakly transonic regime. In the authors' opinion, a very natural and convenient approach for solving the Euler equations governing unsteady compressible flows is provided by the so-called lambda formulation recently developed by Moretti et al.^{1,2}; the time-dependent Euler equations are written as compatibility equations for bicharacteristic variables and discretized using upwind differences to account for the direction of wave propagation phenomena. As such, the lambda formulation combines the physical soundness and intrinsic accuracy of the method of characteristics with the coding simplicity of finite difference schemes and also possesses a well-documented¹⁻⁵ "shock-capturing" capability without any need for artificial dissipation. Unfortunately, these captured shocks are isentropic and can thus be considered satisfactory only in the weakly transonic regime; more importantly, they cannot propagate upstream in the flowfield and their location and strength can depend on the initial conditions and on the scheme used to approach a steady state.⁶ However, such a very serious drawback of the method can be removed either by means of a shock-tracking technique⁷ or by a local correction in the shock region which allows upstream propagation.⁸ Therefore, the lambda formulation, already extremely valuable for computing subcritical flows, is a potential powerful tool also for calculating transonic flows.

Since its first appearance as a working tool for solving compressible flows numerically,¹ the lambda methodology has undergone several improvements. In particular, the authors have developed various implicit integration methods³⁻⁵ in order to overcome the CFL stability limitation of the original explicit integration schemes.^{1,2} Also, when using an orthogonal curvilinear coordinate system for solving two-dimensional problems, a significant improvement in the accuracy has been obtained by employing the incompressible potential flow net as the computational grid.⁴ On the other hand, when computing a compressible flow around an airfoil or inside a cascade using a rather coarse mesh, large spurious

total pressure (entropy) errors are usually generated around the leading and trailing edges, where large flow gradients are induced by the geometry. This difficulty is common to most numerical schemes and is usually reduced to an acceptable level by refining the mesh in the entire flowfield or locally in the regions where large gradients occur.

A different, more sophisticated way of improving the accuracy of a sought numerical solution is provided by the effective use of perturbative variables and equations. For example, in 1972, Davis⁹ obtained very accurate solutions of incompressible viscous flow past a parabola by extracting the inviscid flow solution analytically using a conformal mapping. More recently, Steger¹⁰ suggested solving for the difference between the desired solution and an accurately computed approximation as a means for obtaining a high level of accuracy on a relatively coarse mesh and Chow et al.¹¹ demonstrated the validity of the idea by exploiting a fine-grid solution of the full potential equations to obtain an accurate coarse-grid solution of the Euler equations.

Here, the development of a "perturbative lambda formulation" appears as the most natural and logical development of the method proposed in Ref. 4. In fact, if the incompressible potential flow net is used as the computational grid,⁴ an accurate incompressible flow solution is available at no extra cost and, therefore, it is convenient to reformulate the governing equations in terms of new variables, which are the differences between the unknowns of the compressible problem and the solution of the incompressible flow. In this way, the geometry-induced gradients are accounted for by the known incompressible flow solution and a perturbative problem is obtained that is smoother and better behaved than the original one and can thus be solved accurately even on a coarse mesh.

The proposed approach has been recently applied to solve subsonic and transonic internal flows in one and two dimensions¹²; for the case of one-dimensional flows, in particular, transonic flows characterized by rather strong shocks have been computed very accurately and efficiently, using the shock-tracking procedure of Moretti⁷ and a fully implicit integration scheme. Here, the new perturbative lambda equations for two-dimensional homentropic flows are provided in an orthogonal coordinate system and solved numerically by means of an alternating direction implicit (ADI) method. Finally, results for subcritical and supercritical flows past a NACA 0012 airfoil are presented, which demonstrate the great accuracy improvement of the new approach over the standard lambda methodology.

Received Dec. 4, 1984; revision received June 10, 1985. Copyright © American Institute of Aeronautics and Astronautics, Inc., 1985. All rights reserved.

*Professor, Istituto di Macchine.

†Professor, Istituto di Macchine. Member AIAA.

Governing Equations

For the case of homentropic two-dimensional compressible flows, the lambda formulation equations in a general system of curvilinear orthogonal coordinates are given in Ref. 4 as

$$\begin{aligned} C_t + D_t + \frac{v_1 + a}{h_1} \frac{\partial C}{\partial q_1} + \frac{v_2}{h_2} \frac{\partial C}{\partial q_2} \\ + \frac{v_1 - a}{h_1} \frac{\partial D}{\partial q_1} + \frac{v_2}{h_2} \frac{\partial D}{\partial q_2} \\ = \frac{2v_2}{h_1 h_2} \left(\frac{\partial h_2}{\partial q_1} v_2 - \frac{\partial h_1}{\partial q_2} v_1 \right) \end{aligned} \quad (1)$$

$$\begin{aligned} E_t + F_t + \frac{v_1}{h_1} \frac{\partial E}{\partial q_1} + \frac{v_2 + a}{h_2} \frac{\partial E}{\partial q_2} \\ + \frac{v_1}{h_1} \frac{\partial F}{\partial q_1} + \frac{v_2 - a}{h_2} \frac{\partial F}{\partial q_2} \\ = \frac{2v_1}{h_1 h_2} \left(\frac{\partial h_1}{\partial q_2} v_1 - \frac{\partial h_2}{\partial q_1} v_2 \right) \end{aligned} \quad (2)$$

$$\begin{aligned} \frac{1}{2} \{ C_t - D_t + E_t - F_t \} + \frac{v_1 + a}{h_1} \frac{\partial C}{\partial q_1} - \frac{v_1 - a}{h_1} \frac{\partial D}{\partial q_1} \\ + \frac{v_2 + a}{h_2} \frac{\partial E}{\partial q_2} - \frac{v_2 - a}{h_2} \frac{\partial F}{\partial q_2} \\ = \frac{-2a}{h_1 h_2} \left(\frac{\partial h_2}{\partial q_1} v_1 + \frac{\partial h_1}{\partial q_2} v_2 \right) \end{aligned} \quad (3)$$

$$C - D - E + F = 0 \quad (4)$$

In Eqs. (1-4) the subscript t indicates partial derivatives with respect to time, q_1 , q_2 , h_1 , and h_2 are the orthogonal curvilinear coordinates and the corresponding scale factors, v_1 and v_2 are the two components of the velocity vector V , and C , D , E , and F are the four bicharacteristic variables, namely,

$$C = v_1 + \zeta a \quad (5)$$

$$D = v_1 - \zeta a \quad (6)$$

$$E = v_2 + \zeta a \quad (7)$$

$$F = v_2 - \zeta a \quad (8)$$

with $\zeta = 2/(\gamma - 1)$, γ being the specific heats ratio of the perfect gas under consideration.

In order to obtain a perturbative form of Eqs. (1-4), we need to define an appropriate incompressible flow solution, V' , a' . It is obvious that the incompressible velocity vector V' has to satisfy the following equations:

$$\text{div } V' = \text{curl } V' = 0 \quad (9a,b)$$

according to classical incompressible potential flow theory. However, such a theory is not adequate to provide a suitable speed of sound a' , which would be infinite, insofar as the pressure has a dynamic but no thermodynamic significance. Therefore, an appropriate "incompressible" speed of sound a' is defined here from the following steady total enthalpy equation:

$$v_1'^2 + v_2'^2 + \zeta a'^2 = \zeta a_0^2 \quad (10)$$

where a_0 is the (known) stagnation speed of sound of the compressible flow of interest. It is noteworthy that the incompressible velocity vector V' and speed of sound a' are uncoupled so that a' can be evaluated from the velocity field V' , solution of Eqs. (9), by means of the algebraic relationship [Eq. (10)], much in the same manner as the pressure is obtained by the Bernoulli equation in the case of classical incompressible flow theory. Furthermore, for very low Mach number flows, the speed of sound a tends to a' , so that V' and a' provide a very suitable "incompressible flow solution" for defining the appropriate perturbative bicharacteristic variables \tilde{C} , \tilde{D} , \tilde{E} , and \tilde{F} according to the following relationships:

$$\tilde{C} = C - (v_1' + \zeta a') \quad (11)$$

$$\tilde{D} = D - (v_1' - \zeta a') \quad (12)$$

$$\tilde{E} = E - (v_2' + \zeta a') \quad (13)$$

$$\tilde{F} = F - (v_2' - \zeta a') \quad (14)$$

By eliminating C , D , E , and F in terms of the corresponding perturbative variables \tilde{C} , \tilde{D} , \tilde{E} , and \tilde{F} , Eqs. (1-4), after some lengthy algebra, provide the general perturbative lambda equations in two dimensions, as

$$\begin{aligned} \tilde{C}_t + \tilde{D}_t + \frac{v_1 + a}{h_1} \frac{\partial \tilde{C}}{\partial q_1} + \frac{v_2}{h_2} \frac{\partial \tilde{C}}{\partial q_2} + \frac{v_1 - a}{h_1} \frac{\partial \tilde{D}}{\partial q_1} + \frac{v_2}{h_2} \frac{\partial \tilde{D}}{\partial q_2} \\ = \frac{2\tilde{v}_2}{h_1 h_2} \left(\frac{\partial h_2}{\partial q_1} \tilde{v}_2 - \frac{\partial h_1}{\partial q_2} \tilde{v}_1 \right) - k_{1,1} \tilde{v}_1 - k_{2,1} \tilde{v}_2 - k_{3,1} \tilde{a} \end{aligned} \quad (15)$$

$$\begin{aligned} E_t + F_t + \frac{v_1}{h_1} \frac{\partial E}{\partial q_1} + \frac{v_2 + a}{h_2} \frac{\partial E}{\partial q_2} + \frac{v_1}{h_1} \frac{\partial \tilde{F}}{\partial q_1} + \frac{v_2 - a}{h_2} \frac{\partial \tilde{F}}{\partial q_2} \\ = \frac{2\tilde{v}_1}{h_1 h_2} \left(\frac{\partial h_1}{\partial q_2} \tilde{v}_1 - \frac{\partial h_2}{\partial q_1} \tilde{v}_2 \right) - k_{2,1} \tilde{v}_1 - k_{1,2} \tilde{v}_2 - k_{3,2} \tilde{a} \end{aligned} \quad (16)$$

$$\begin{aligned} \frac{1}{2} \{ \tilde{C}_t - \tilde{D}_t + \tilde{E}_t - \tilde{F}_t \} + \frac{v_1 + a}{h_1} \frac{\partial \tilde{C}}{\partial q_1} - \frac{v_1 - a}{h_1} \frac{\partial \tilde{D}}{\partial q_1} \\ + \frac{v_2 + a}{h_2} \frac{\partial \tilde{E}}{\partial q_2} - \frac{v_2 - a}{h_2} \frac{\partial \tilde{F}}{\partial q_2} \\ = - \frac{2\tilde{a}}{h_1 h_2} \left(\frac{\partial h_2}{\partial q_1} \tilde{v}_1 + \frac{\partial h_1}{\partial q_2} \tilde{v}_2 \right) - k_{4,1} \tilde{v}_1 - k_{4,2} \tilde{v}_2 - k_5 \end{aligned} \quad (17)$$

$$\tilde{C} - \tilde{D} - \tilde{E} + \tilde{F} = 0 \quad (18)$$

where \tilde{v}_1 , \tilde{v}_2 , and \tilde{a} are the differences between the corresponding compressible and incompressible flow variables and the k coefficients are functions only of the incompressible flow solution and of the coordinate system, so that they are constant with respect to time and are given as

$$k_{1,i,j} = \frac{2}{h_i} \left(\frac{\partial h_i}{\partial q_j} \frac{v_j'}{h_j} + \frac{\partial v_i'}{\partial q_i} \right) \quad (19)$$

$$k_{2,i,j} = \frac{2}{h_j} \left(\frac{h_j}{h_i} \frac{\partial v_j'}{\partial q_i} - \frac{\partial h_j}{\partial q_i} \frac{v_j'}{h_i} \right) \quad (20)$$

$$k_{3,i} = \frac{2\zeta}{h_i} \frac{\partial a'}{\partial q_i} \quad (21)$$

$$k_{4,i,j} = \frac{2}{h_i} \left(\zeta \frac{\partial a'}{\partial q_i} + \frac{\partial h_j}{\partial q_i} \frac{a'}{h_j} \right) \quad (22)$$

$$k_5 = 2\zeta \left(\frac{\partial a'}{\partial q_1} \frac{v_1'}{h_1} + \frac{\partial a'}{\partial q_2} \frac{v_2'}{h_2} \right) \quad (23)$$

It must be emphasized that the perturbative equations (15-18) preserve the basic structure of the standard (lambda) equations (1-4), with additional terms containing the unknown perturbative variables only as linear source (undifferentiated) terms. Also, the coefficients of the bicharacteristic-type advection terms contain the full compressible flow variables v_1 , v_2 , and a ; as such, they provide the slopes of the physical bicharacteristic lines along which disturbances propagate and thus the direction of the upwind differences to be used for discretizing the associated spatial derivatives. Therefore, Eqs. (15-18) are suitable to be solved numerically, without any additional difficulty, by means of any technique developed for the standard lambda equations (1-4) and, in particular, by any of the implicit methods proposed by the authors.³⁻⁵

Numerical Method

The numerical method employed in this study is a simplified version of the ADI technique provided in Ref. 4. Equations (15-18) are discretized in time by means of a two-level Euler time stepping, using the delta approach,¹³ with only the derivatives of the bicharacteristic variables in Eqs. (15-17) and all of the terms in Eq. (18) being evaluated at the new time level, to give

$$\begin{aligned} \frac{\Delta C}{\Delta t} + \frac{\Delta D}{\Delta t} + \frac{(v_1 + a)^n}{h_1} \frac{\partial \Delta C}{\partial q_1} + \frac{v_2^n}{h_2} \frac{\partial \Delta C}{\partial q_2} \\ + \frac{(v_1 - a)^n}{h_1} \frac{\partial \Delta D}{\partial q_1} + \frac{v_2^n}{h_2} \frac{\partial \Delta D}{\partial q_2} = \text{SSEQN}(15)^n \end{aligned} \quad (24)$$

$$\begin{aligned} \frac{\Delta E}{\Delta t} + \frac{\Delta F}{\Delta t} + \frac{v_1^n}{h_1} \frac{\partial \Delta E}{\partial q_1} + \frac{(v_2 + a)^n}{h_2} \frac{\partial \Delta E}{\partial q_2} \\ + \frac{v_1^n}{h_1} \frac{\partial \Delta F}{\partial q_1} + \frac{(v_2 - a)^n}{h_2} \frac{\partial \Delta F}{\partial q_2} = \text{SSEQN}(16)^n \end{aligned} \quad (25)$$

$$\begin{aligned} \frac{1}{2} \left\{ \frac{\Delta C}{\Delta t} - \frac{\Delta D}{\Delta t} + \frac{\Delta E}{\Delta t} - \frac{\Delta F}{\Delta t} \right\} + \frac{(v_1 + a)^n}{h_1} \frac{\partial \Delta C}{\partial q_1} \\ - \frac{(v_1 - a)^n}{h_1} \frac{\partial \Delta D}{\partial q_1} + \frac{(v_2 + a)^n}{h_2} \frac{\partial \Delta E}{\partial q_2} \\ - \frac{(v_2 - a)^n}{h_2} \frac{\partial \Delta F}{\partial q_2} = \text{SSEQN}(17)^n \end{aligned} \quad (26)$$

$$\Delta C - \Delta D - \Delta E + \Delta F = 0 \quad (27)$$

Here, $\text{SSEQN}(N)^n$ is shorthand notation for the steady-state part of Eq. (N) evaluated at the old time level t^n , Δt the time step, $\Delta C = \bar{C}^{n+1} - \bar{C}^n$, etc., the superscripts $n+1$ and n indicating the new and old time levels, $t^{n+1} = t^n + \Delta t$ and t^n . In Refs. 3 and 4, the terms of the type $(v_1 + a)$ were also evaluated at the new time level (implicitly) and the equations were then linearized using the delta approach¹³ and neglecting terms of order Δ^2 . However, in Ref. 12, it has been verified numerically that the present simpler approach converges in a slightly greater number of iterations but requires less CPU time due to the reduced amount of computing to be performed at every time level. Notice also that the additional terms introduced by the perturbative formulation are evaluated explicitly, with the k coefficients being computed once and for all at the beginning of the calculation.

Equations (24-26) are then discretized in space using two-point, first-order-accurate upwind differences for all of the spatial derivatives of the incremental variables (in the left-

hand sides), to give

$$\begin{aligned} \frac{\Delta C_{i,j}}{\Delta t} + \frac{\Delta D_{i,j}}{\Delta t} + \frac{(v_1 + a)^n}{h_1} \frac{\Delta C_{i,j} - \Delta C_{i-1,j}}{\Delta q_1} \\ + \frac{v_2^n + |v_2^n|}{2h_2} \frac{\Delta C_{i,j} - \Delta C_{i,j-1}}{\Delta q_2} \\ + \frac{v_2^n - |v_2^n|}{2h_2} \frac{\Delta C_{i,j+1} - \Delta C_{i,j}}{\Delta q_2} \\ + \frac{(v_1 - a)^n + |(v_1 - a)^n|}{2h_1} \frac{\Delta D_{i,j} - \Delta D_{i-1,j}}{\Delta q_1} \\ + \frac{(v_1 - a)^n - |(v_1 - a)^n|}{2h_1} \frac{\Delta D_{i+1,j} - \Delta D_{i,j}}{\Delta q_1} \\ + \frac{v_2^n + |v_2^n|}{2h_2} \frac{\Delta D_{i,j} - \Delta D_{i,j-1}}{\Delta q_2} \\ + \frac{v_2^n - |v_2^n|}{2h_2} \frac{\Delta D_{i,j+1} - \Delta D_{i,j}}{\Delta q_2} = \text{SSEQN}(15)^n \end{aligned} \quad (28)$$

$$\begin{aligned} \frac{\Delta E_{i,j}}{\Delta t} + \frac{\Delta F_{i,j}}{\Delta t} + \frac{v_1^n}{h_1} \frac{\Delta E_{i,j} - \Delta E_{i-1,j}}{\Delta q_1} \\ + \frac{(v_2 + a)^n}{h_2} \frac{\Delta E_{i,j} - \Delta E_{i,j-1}}{\Delta q_2} \\ + \frac{v_1^n}{h_1} \frac{\Delta F_{i,j} - \Delta F_{i-1,j}}{\Delta q_1} \\ + \frac{(v_2 - a)^n}{h_2} \frac{\Delta F_{i,j+1} - \Delta F_{i,j}}{\Delta q_2} = \text{SSEQN}(16)^n \end{aligned} \quad (29)$$

$$\begin{aligned} \frac{1}{2\Delta t} \{ \Delta C_{i,j} - \Delta D_{i,j} + \Delta E_{i,j} - \Delta F_{i,j} \} \\ + \frac{(v_1 + a)^n}{h_2} \frac{\Delta C_{i,j} - \Delta C_{i-1,j}}{\Delta q_1} \\ - \frac{(v_1 - a)^n + |(v_1 - a)^n|}{2h_1} \frac{\Delta D_{i,j} - \Delta D_{i-1,j}}{\Delta q_1} \\ - \frac{(v_1 - a)^n - |(v_1 - a)^n|}{2h_1} \frac{\Delta D_{i+1,j} - \Delta D_{i,j}}{\Delta q_1} \\ + \frac{(v_2 + a)^n}{h_2} \frac{\Delta E_{i,j} - \Delta E_{i,j-1}}{\Delta q_2} \\ - \frac{(v_2 - a)^n}{h_2} \frac{\Delta F_{i,j+1} - \Delta F_{i,j}}{\Delta q_2} = \text{SSEQN}(17)^n \end{aligned} \quad (30)$$

$$\Delta C_{i,j} - \Delta D_{i,j} - \Delta E_{i,j} + \Delta F_{i,j} = 0 \quad (31)$$

In Eqs. (28-30), it is assumed that the streamwise velocity component v_1 is always positive and that the absolute value of the transversal velocity component v_2 is always lower than the speed of sound a . These hypotheses are true in most inviscid flows of practical interest; however, finite difference equations based on more general upwind differences can be derived very straightforwardly. Also, the subscripts i and j , indicating the longitudinal and transversal gridpoint locations respectively, are omitted in all the coefficients for notational simplicity. As far as the right-hand sides of Eqs. (28-30) are concerned, three-point, second-order-accurate upwind dif-

ferences are used for all of the spatial derivatives of the bicharacteristic variables, whereas standard central differences approximate the spatial derivatives of the scale factors. In this way, at convergence the final (steady-state) solution is second-order-accurate.

All of the $\Delta F_{i,j}$ variables in Eqs. (28-30) are finally eliminated, by means of Eq. (31), in favor of $\Delta C_{i,j}$, $\Delta D_{i,j}$, and $\Delta E_{i,j}$ to provide a large linear 3×3 block pentadiagonal system. Such a system is factorized by means of a two-sweep ADI method, so that an approximate solution for $\Delta C_{i,j}$, $\Delta D_{i,j}$, and $\Delta E_{i,j}$ is obtained by simply solving a 3×3 block tridiagonal system along each row and column of the computational domain.⁴

As far as the boundary conditions are concerned, they take a particularly simple form insofar as they refer to the perturbative variables and also because the computational grid is always chosen to coincide with the flow net of the incompressible flow V' . At the body surface (or symmetry line), which is aligned with the coordinate line q_1 , the no-injection boundary condition is given by $\bar{v}_2 = 0$. The outer boundary is divided into an inlet boundary and an outlet boundary (ahead of and behind the airfoil), coinciding with incompressible flow potential lines and one or two far-field boundaries (above and below the airfoil), coinciding with incompressible flow streamlines for symmetric and asymmetric flows, respectively (see, e.g., Fig. 1). For the case of the subsonic freestream flows of interest here, two boundary conditions need to be prescribed at the inlet boundary, namely, the direction of the velocity vector V , which is obviously assumed to be parallel to V' , and the total enthalpy (speed of sound). These two conditions are given as

$$\bar{v}_2 = 0 \quad (32)$$

and

$$\zeta \bar{a}^2 + \bar{v}_1^2 + 2\zeta \bar{a}' \bar{a} + 2v_1' \bar{v}_1 = 0 \quad (33)$$

A single boundary condition is needed instead at the outlet boundary, where the static pressure (i.e., \bar{a}) is assigned, and at the far-field boundaries, where the impermeability condition with respect to the incompressible flow streamline, $\bar{v}_2 = 0$, is enforced.

At all of the boundary gridpoints, the number of boundary conditions (which are all physical ones) is exactly equal to the

number of derivatives of the bicharacteristic variables whose upwind differences would require gridpoints external to the computational domain. The governing equations are thus linearly combined to eliminate such derivatives and coupled with the boundary conditions to provide four equations for the four unknowns \bar{C} , \bar{D} , \bar{E} , and \bar{F} . For example, at the outlet boundary, the derivative of the variable \bar{D} with respect to q_1 is eliminated from Eqs. (24) and (26) and the resulting equation is used together with the pressure boundary condition and Eqs. (25) and (27). At the inlet boundary, the two aforementioned physical boundary conditions are used together with Eq. (27) and the equation obtained by combining Eqs. (24) and (26) so as to eliminate the derivative of \bar{C} with respect to q_1 [Eq. (25), which contains derivatives of \bar{E} and \bar{F} with respect to q_1 , whose upwind discretizations all require points external to the computational domain, is discarded altogether].

It seems appropriate at this point to remark that the perturbative approach provides a further advantage over the standard method of Ref. 4; namely, it allows to impose the outer boundary conditions closer to the body, insofar as the compressibility effects (which are solved for) become negligible at a much smaller distance from the airfoil than that required for the entire (compressible) flow to approach freestream conditions. Also, the computational grid employed by both methods is the same potential flow net and provides the incompressible flow velocity field at no extra cost. Therefore, the present perturbative approach does not require any significant increase in the computational effort with respect to its standard parent.⁴ As a matter of fact, at every time step, only 8 multiplications and 12 additions per gridpoint have to be performed to compute the additional terms in the right-hand sides of Eqs. (28-30) and to update the extra dependent variables v_1 , v_2 ; and a ; a negligible effort indeed for the present case of an implicit method.

The initial condition for the calculations presented in the next section is the incompressible flow solution V' , a' , so that all the perturbative variables are zero at the initial time level. The incompressible flow solution for V' , as well as the com-

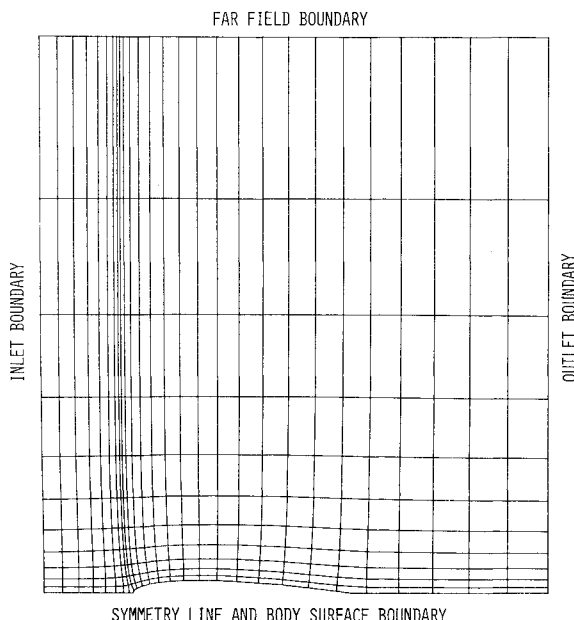


Fig. 1 Computational mesh for symmetric flow.

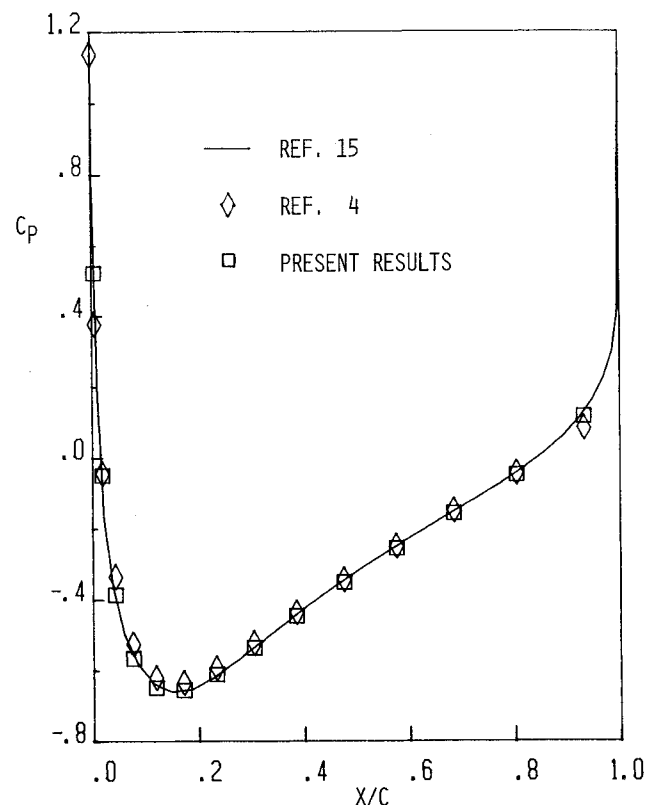


Fig. 2 Pressure coefficient results for symmetric flow at $M_0 = 0.72$.

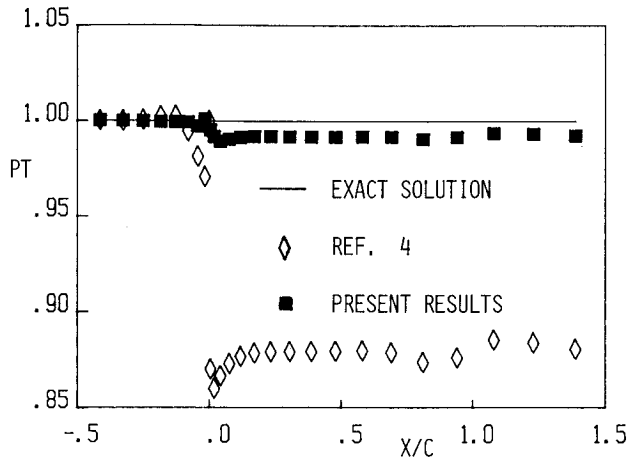


Fig. 3 Total pressure results for symmetric flow at $M_0 = 0.72$.

putational grid and its scale factors, are computed using the numerical integration of the Schwartz-Christoffel transformation due to Davis.¹⁴

Results

The present perturbative approach has been developed as a very effective tool for reducing the large total pressure (entropy) errors around stagnation points suffered by most numerical methods when using rather coarse meshes. Therefore, flow past a NACA 0012 airfoil has been chosen as a very suitable test problem to assess the validity of the proposed methodology and also because of the large amount of numerical results available in the literature. Symmetric flow at a freestream Mach number M_0 equal to 0.72 has been considered at first, using the rather coarse 27×11 nonuniform (potential flow net) mesh depicted in Fig. 1.

It seems appropriate to emphasize at this point that there is no need for a q_2 (the incompressible potential function) coordinate line to pass through each stagnation point, a necessary requirement for the method of Ref. 4, because only the smooth compressibility effects are solved for and the perturbative variables can be differenced across a stagnation point without any numerical difficulty.

The present results are given in Fig. 2 as the pressure coefficient C_p distribution along the surface of the airfoil. The very accurate solution due to Lock¹⁵ is also given for comparison and is seen to coincide with the present coarse-mesh solution, for all practical purposes. In the same figure, the results obtained using the standard lambda method of Ref. 4 and the present mesh (locally modified near the leading edge to allow for an extra q_2 line passing through it) are also provided. From the results of Fig. 2, it would appear that the perturbative approach provides only a minor improvement over an already extremely accurate standard lambda method. However, a very different conclusion emerges from Fig. 3, where the corresponding total pressure (PT) distributions along the symmetry line and along the surface of the airfoil are plotted vs the exact solution, $PT=1$. Whereas the total pressure errors of the present approach are extremely small (always less than 1%) and very satisfactory, those of the standard lambda method of Ref. 4 are much greater (up to 10% or even more) and certainly not acceptable.

In conclusion, when using a rather coarse mesh such as the present one, the new perturbative approach provides a very satisfactory solution overall, whereas the standard lambda method computes the pressure field satisfactorily, but the velocity field inaccurately, as the excessive total pressure errors indicate. And, in fact, by comparing the Mach number distributions along the surface of the airfoil obtained using both methods with the reference solution of Lock,¹⁵ as in Fig. 4, the superiority of the perturbative approach over the standard lambda method is paramount.

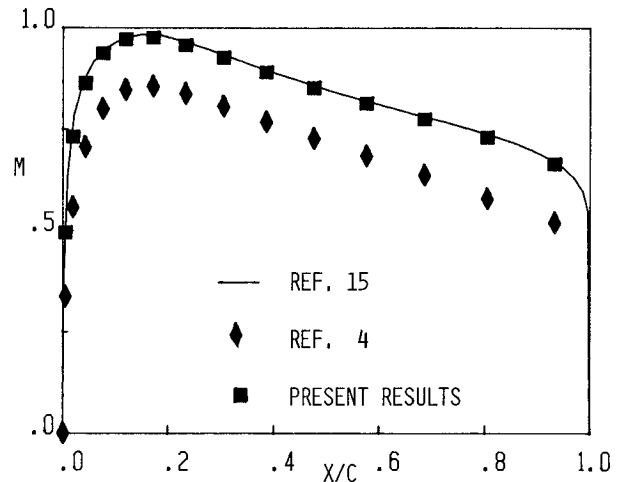


Fig. 4 Mach number results for symmetric flow at $M_0 = 0.72$.

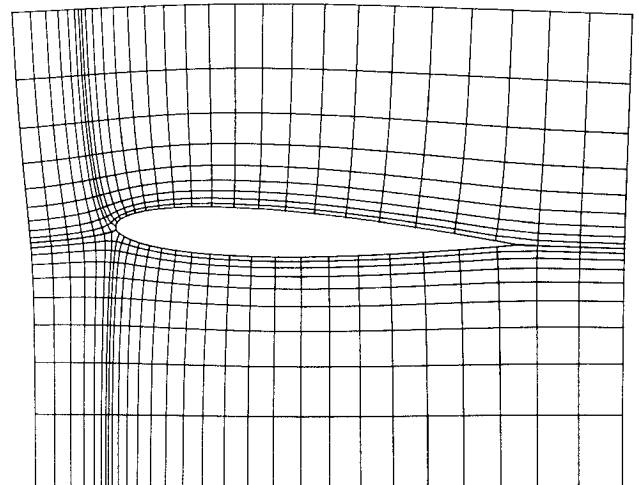


Fig. 5 Near field computational mesh for flow at $\alpha = 3$ deg.

Of course, one may argue that the pressure coefficient (which provides the lift and drag on the airfoil) is the most important property to be computed and, therefore, the improvement due to the perturbative approach is minor. However, when considering lifting airfoils (e.g., the same NACA 0012 airfoil at a nonzero angle of attack), the method of Ref. 4 cannot be employed insofar as it requires the stagnation point position to coincide with a computational gridpoint. On the other hand, in the new perturbative approach, the stagnation point can be positioned anywhere inside a mesh. Therefore, it can be anticipated that a very accurate solution can be obtained if the stagnation point does not move outside such a mesh, due to compressibility effects. From this viewpoint, it turns out that the high accuracy of the method (which allows to use rather coarse meshes) also extends the range of freestream Mach numbers and/or angles of attack for which a reliable solution can be obtained.

In order to verify the capability of the method to compute flows in which the leading-edge stagnation point is not known a priori, subcritical flows past a NACA 0012 airfoil, characterized by $M_0 = 0.63$ and an angle of attack $\alpha = 2$ deg and by $M_0 = 0.50$, $\alpha = 3$ deg, have been considered using a slightly finer $39 \times 14 \times 2$ mesh, whose near field is depicted in Fig. 5 for the case $\alpha = 3$ deg. For such computations, it has been necessary to extend the computational domain up to 3.5 chord lengths above and below the airfoil in order to obtain results independent of the far-field boundary conditions. The

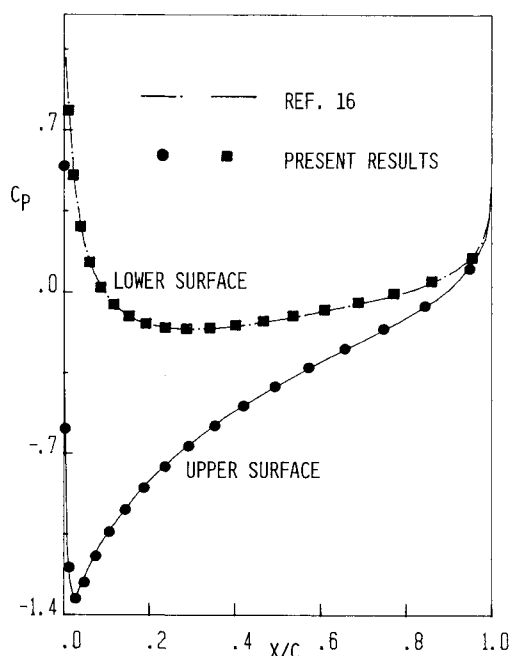


Fig. 6 Pressure coefficient results for flow at $M_0 = 0.50$, $\alpha = 3$ deg.

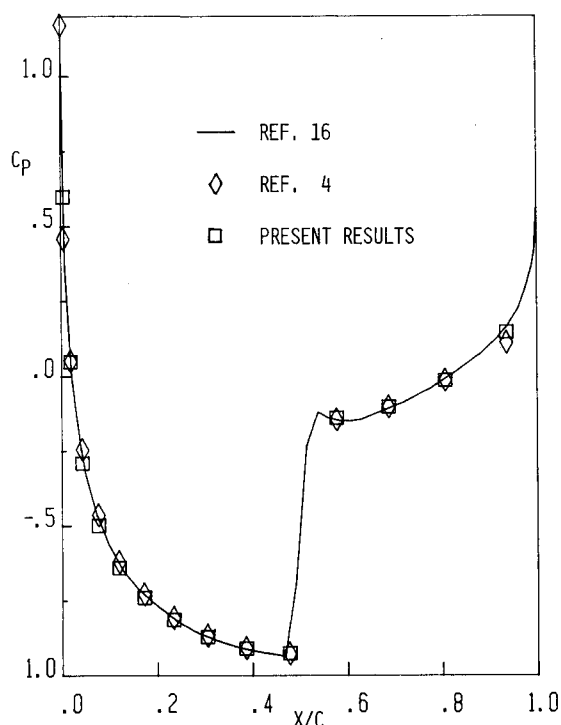


Fig. 7 Pressure coefficient results for symmetric flow at $M_0 = 0.80$.

pressure coefficient distributions on both sides of the airfoil computed using the present method are given in Fig. 6 for the second flow case together with the very accurate solutions of Jameson.¹⁶ The agreement is excellent, demonstrating once again the remarkable accuracy of the proposed approach. The results for the $M_0 = 0.63$, $\alpha = 2$ deg flow case have comparable accuracy and are therefore omitted. Furthermore, the total pressure errors along the surface of the airfoil are always less than 1% in both cases, demonstrating that both pressure and velocity are computed accurately.

Finally, in order to test the proposed methodology even beyond the limits of its theoretical validity, symmetric weakly transonic ($M_0 = 0.80$) flow past a NACA 0012 airfoil was considered using the same coarse mesh of Fig. 1. The pressure coefficient distributions, computed using both the present method and the standard lambda approach of Ref. 4, are plotted in Fig. 7 together with the very accurate results due to Jameson,¹⁶ who solved the Euler equations in conservation form on a very fine 128×32 mesh. Once again, it appears that the perturbative approach provides an accuracy improvement (especially near the trailing edge of the airfoil) over the already remarkable results of Ref. 4. However, it must be emphasized once more that the present approach cannot be considered reliable for computing transonic flows, unless supplemented by a shock-tracking procedure⁷ or any other suitable mechanism for upstream propagation through the shocks.⁸

As far as the efficiency of the calculations is concerned, a satisfactory convergence has always been obtained in less than 100 iterations (time steps) using a local CFL number of 10-15, the CPU time (on a HP 9000/9040 minicomputer) being about 5 and 18 min for the computations using the 27×11 and $39 \times 14 \times 2$ meshes, respectively. Such a convergence rate is very similar to that of the method of Ref. 4, when applicable.

Conclusions

A perturbative lambda formulation has been provided that uses an available accurate incompressible flow solution and computes only the compressibility effects, so that extremely accurate results for the complete compressible flow problem are obtained even on a relatively coarse mesh. Although the perturbative problem is not necessarily a small correction, it is always smoother than the original one, especially around the stagnation points, where compressibility effects are small but large geometry-induced gradients are present. Therefore, the numerical results obtained using the proposed perturbative approach are considerably more accurate, particularly with respect to the critical total pressure errors, than those obtained using the corresponding standard method and the same mesh.

Acknowledgments

The present research has been supported by Ministero della Pubblica Istruzione and by Consiglio Nazionale delle Ricerche. The idea of a perturbative lambda formulation was born during a very stimulating discussion among the authors and Prof. R. T. Davis, at the University of Cincinnati in July 1982.

References

- Moretti, G., "The λ -Scheme," *Computers and Fluids*, Vol. 7, 1979, pp. 191-205.
- Zannetti, L. and Colasurdo, G., "Unsteady Compressible Flow: A Computational Method Consistent with the Physical Phenomena," *AIAA Journal*, Vol. 19, July 1981, pp. 851-856.
- Dadone, A. and Napolitano, M., "An Implicit Lambda Scheme," *AIAA Journal*, Vol. 21, Oct. 1983, pp. 1391-1399.
- Dadone, A. and Napolitano, M., "Efficient Transonic Flow Solutions to the Euler Equations," *AIAA Paper 83-0258* 1983 (also, "An Efficient ADI Lambda Formulation," *Computers and Fluids*, Vol. 13, 1985, pp. 383-395).
- Napolitano, M. and Dadone A., "Implicit Lambda Methods for Three-Dimensional Compressible Flows," *AIAA Journal*, Vol. 23, Sept. 1985, pp. 1343-1347.
- Chakravarti, S. R., Anderson, D. A., and Salas, M. D., "The Split Coefficient Matrix Method for Hyperbolic Systems of Gasdynamic Equations," *AIAA Paper 80-0268*, 1980.
- Moretti, G., "Fast Euler Solver for Steady, One-dimensional Flows," NASA CR 3689, 1983 (also, *Computers and Fluids*, Vol. 13, 1985, pp. 61-81).

⁸Dadone, A. and Magi, V., "A Quasi-Conservative Lambda Formulation," AIAA Paper 85-0088, 1985.

⁹Davis, R. T., "Numerical Solution of the Navier-Stokes Equations for Symmetric Laminar Incompressible Flow Past a Parabola," *Journal of Fluid Mechanics*, Vol. 59, No. 3, 1972, pp. 417-433.

¹⁰Steger, J. L., "On Application of Body Conforming Curvilinear Grids for Finite Difference Solutions of External Flow," *Numerical Grid Generation*, edited by J. F. Thompson, North Holland Publishing Co., Amsterdam, 1982, pp. 295-316.

¹¹Chow, L. J., Pulliam, T. H., and Steger, J. L., "A General Perturbation Approach for the Equations of Fluid Dynamics," AIAA Paper 83-1903, 1983.

¹²Dadone, A. and Napolitano, M., "Accurate and Efficient Solutions of Compressible Internal Flows," *Journal of Propulsion and Power*, Vol. 1, pp. 456-463.

¹³Beam, R. M. and Warming, R. F., "An Implicit Factored Scheme for the Compressible Navier-Stokes Equations," *AIAA Journal*, Vol. 16, April 1978, pp. 393-402.

¹⁴Davis, R. T., "Notes on Numerical Methods for Coordinate Generation Based on a Mapping Technique," *von Kármán Institute Lecture Series 1981-5*, March 30-April 3, 1981.

¹⁵Lock, R. C., "Test Cases for Numerical Methods in Two-Dimensional Transonic Flows," AGARD-R575-70, 1970.

¹⁶Jameson, A., "Solution of the Euler Equations by a Multigrid Method," *Applied Mathematics and Computation*, Vol. 13, 1983, pp. 327-356.

From the AIAA Progress in Astronautics and Aeronautics Series

RAREFIED GAS DYNAMICS—v. 74 (Parts I and II)

Edited by Sam S. Fisher, University of Virginia

The field of rarefied gas dynamics encompasses a diverse variety of research that is unified through the fact that all such research relates to molecular-kinetic processes which occur in gases. Activities within this field include studies of (a) molecule-surface interactions, (b) molecule-molecule interactions (including relaxation processes, phase-change kinetics, etc.), (c) kinetic-theory modeling, (d) Monte-Carlo simulations of molecular flows, (e) the molecular kinetics of species, isotope, and particle separating gas flows, (f) energy-relaxation, phase-change, and ionization processes in gases, (g) molecular beam techniques, and (h) low-density aerodynamics, to name the major ones.

This field, having always been strongly international in its makeup, had its beginnings in the early development of the kinetic theory of gases, the production of high vacuums, the generation of molecular beams, and studies of gas-surface interactions. A principal factor eventually solidifying the field was the need, beginning approximately twenty years ago, to develop a basis for predicting the aerodynamics of space vehicles passing through the upper reaches of planetary atmospheres. That factor has continued to be important, although to a decreasing extent; its importance may well increase again, now that the USA Space Shuttle vehicle is approaching operating status.

A second significant force behind work in this field is the strong commitment on the part of several nations to develop better means for enriching uranium for use as a fuel in power reactors. A third factor, and one which surely will be of long term importance, is that fundamental developments within this field have resulted in several significant spinoffs. A major example in this respect is the development of the nozzle-type molecular beam, where such beams represent a powerful means for probing the fundamentals of physical and chemical interactions between molecules.

Within these volumes is offered an important sampling of rarefied gas dynamics research currently under way. The papers included have been selected on the basis of peer and editor review, and considerable effort has been expended to assure clarity and correctness.

Published in 1981, 1224 pp., 6×9, illus., \$65.00 Mem., \$109.00 List

TO ORDER WRITE: Publications Dept., AIAA, 1633 Broadway, New York, N.Y. 10019